[21] J. Khan, J.S. Wei, M. Ringner, L.H. Saal, M. Ladanyi, F. Westermann, et al., Classification and diagnostic prediction of cancers using gene expression profiling and artificial neural networks, Nat. Med. 7 (2001) 673–679.
[22] Y. Yamanaka, Y. Hamazaki, Y. Sato, K. Ito, K. Watanabe, T. Heike, et al., Maturational sequence of neuroblastoma revealed by molecular analysis on cDNA microarrays, Int. J. Oncol. 21 (2002) 803–807.
[23] B. Berwanger, O. Hartmann, E. Bergmann, S. Bernard, D. Nielsen, M. Krause, et al., Loss of a FYN-regulated differentiation and growth arrest pathway in advanced stage neuroblastoma, Cancer Cell 2 (2002) 377–386.
[24] J. Takita, M. Ishii, S. Tsutsumi, Y. Tanaka, K. Kato, Y. Toyoda, et al., Gene expression profiling and identification of novel prognostic marker genes in neuroblastoma, Genes Chromosomes Cancer 40 (2004) 120–132.
[25] E. Hiyama, K. Hiyama, H. Yamaoka, T. Sueda, C.P. Reynolds, T. Yokoyama, Expression profiling of favorable and unfavorable neuroblastomas, Pediatr. Surg. Int. 20 (2004) 33–38.
[26] L. McArdle, M. McDermott, R. Purcell, D. Grehan, A. O'Meara, F. Breatnach, et al., Oligonucleotide microarray analysis of gene expression in neuroblastoma displaying loss of chromosome 11q, Carcinogenesis 25 (2004) 1599–1609.
[27] I. Janoueix-Lerosey, E. Novikov, M. Monteiro, N. Gruel, G. Schleiermacher, B. Loriod, et al., Gene expression profiling of 1p35-36 genes in neuroblastoma, Oncogene 23 (2004) 5912–5922.
[28] J.S. Wei, B.T. Greer, F. Westermann, S.M. Steinberg, C.G. Son, Q.R. Chen, et al., Prediction of clinical outcome using gene expression profiling and artificial neural networks for patients with neuroblastoma, Cancer Res. 64 (2004) 6883–6891.
[29] M. Ohira, S. Oba, Y. Nakamura, E. Isogai, S. Kaneko, A. Nakagawa, et al., Expression profiling using a tumor-specific cDNA microarray prediols the prognosis of intermediate-risk neuroblastomas, Cancer Cell 7 (2005) 337-350.
[30] M. Abe, M. Ohira, A. Kaneda, Y. Yagi, S. Yamamoto, Y. Kitano, et al., CpG island methylator phenotype is a strong determinant of poor prognosis in neuroblastomas, Cancer Res., 65 (2005) 828–834.

Oncogene (2005), 1–12

www.nature.com/onc

ORIGINAL PAPER

topors, a p53 and topoisomerase I-binding RING finger protein, is a coactivator of p53 in growth suppression induced by DNA damage

Ling Lin[1,2,3], Toshinori Ozaki[4], Yuki Takada[1,2], Hajime Kageyama[4], Yoko Nakamura[4], Akira Hata[5], Jian-Hua Zhang[3], William F Simonds[3], Akira Nakagawara[4] and Haruhiko Koseki*[,1,2]

[1]*Department of Molecular Embryology, Graduate School of Medicine, Chiba University, 1-8-1 Inohana, Chuo-ku, Chiba 260-8670, Japan;* [2]*RIKEN Research Center for Allergy and Immunology, RIKEN Yokohama Institute, 1-7-22 Suehiro, Tsurumi-ku, Yokohama 230-0045, Japan;* [3]*Metabolic Diseases Branch, National Institute of Diabetes, Digestive and Kidney Diseases, NIH, Bethesda, MD 20892, USA;* [4]*Division of Biochemistry, Chiba Cancer Center Research Institute, 666-2 Nitona, Chuoh-ku, Chiba 260-8717, Japan;* [5]*Department of Public health, Graduate School of Medicine, Chiba University, 1-8-1 Inohana, Chuo-ku, Chiba 260-8670, Japan*

The RING family zinc-finger protein topors (topoisomerase I-binding protein) binds not only topoisomerase I, but also p53 and the AAV-2 Rep78/68 proteins. topors maps to human chromosome 9p21, which contains candidate tumor suppressor genes implicated in small cell lung cancers. In this study, we isolated the murine counterpart of topors and investigated its impact on p53 function. The deduced amino-acid sequence of mouse topors exhibits extensive similarity to human topors. Overexpressed myc-tagged topors associates with and stabilizes p53, and enhances the p53-dependent transcriptional activities of *p21*^{Waf1}, *MDM2* and *Bax* promoters and elevates endogenous *p21*^{Waf1} mRNA levels. Overexpression of topors consequently results in the suppression of cell growth by cell cycle arrest and/or by the induction of apoptosis. Taken together, these studies identify topors as a positive regulator of p53. The expression of *topors* is induced by exposure to the genotoxic reagents cisplatin and camptothecin, a DNA topoisomerase I inhibitor. We therefore postulate that topors mediates p53-dependent cellular responses induced by DNA damage, suggesting its physiological role as a tumor suppressor.
Oncogene advance online publication, 28 February 2005; doi:10.1038/sj.onc.1208554

Keywords: topors; p53; tumor suppressor; DNA damage; cell cycle; apoptosis

Introduction

The p53 tumor suppressor protein is defined as the guardian of the genome, and more than half of all human cancers are characterized by either the loss of the p53 protein or by mutations in its gene (Lane, 1992; Ko and Prives, 1996). The p53 protein comprises 393 amino acids including an amino-terminal transactivation domain, a sequence-specific DNA-binding domain and a multifunctional carboxyl-terminal domain. p53 is involved in the regulation of the cell cycle, apoptosis, senescence, DNA repair, cell differentiation and angiogenesis (Levine, 1997; Vogelstein *et al.*, 2000). These activities of p53 are mediated by one or more known mechanisms including the transcriptional regulation of target genes, functional regulation of interacting proteins, DNA annealing and exonuclease activity. p53 is activated by several stress conditions including DNA damage, the expression of several oncogene products, changes in cellular adhesion and redox potential, and reduction in the ribonucleoside triphosphate pool. In response to such stress signals, p53 undergoes extensive post-translational modification that modulates its stability and activity. The stabilization of p53 is presumed to play a major role in its activation, while modifications unrelated to p53 stabilization may regulate its specific activity (Sionov and Haupt, 1999; Vogelstein *et al.*, 2000). The stability of p53 is tightly regulated by multiple positive and negative feedback loops involving a number of p53 interacting proteins (Sionov and Haupt, 1999; Vogelstein *et al.*, 2000).

Human topoisomerase I-binding protein (h-topors) was first identified by yeast two-hybrid screening as a protein that interacts with human topoisomerase I (hTop1), and turned out to be identical to a novel p53-binding protein, p53BP3 (Haluska *et al.*, 1999; Zhou *et al.*, 1999). An identical protein was also isolated as the DNA-binding protein LUN, as a protein that interacts with adeno-associated virus type 2 (AAV-2) Rep78/68 proteins and as a protein binding to the interferon-inducible large GTPase Mx1 (Chu *et al.*, 2001; Engelhardt *et al.*, 2001; Weger *et al.*, 2002). h-topors is predicted to contain 1045 amino acids and to encode a RING family zinc-finger domain, a putative leucine zipper (LZ) domain, five sequences rich in proline, glutamine, serine and threonine (PEST sequences), an arginine/serine-rich (RS) domain and a bipartite nuclear localization signal (NLS). h-topors is

*Correspondence: H Koseki, RIKEN Research Center for Allergy and Immunology, RIKEN Yokohama Institute, 1-7-22 Suehiro, Tsurumi-ku, Yokohama 230-0045, Japan; E-mail: koseki@rcai.riken.jp
Received 1 June 2004; revised 18 January 2005; accepted 18 January 2005

modified by conjugation to the small ubiquitin-like modifier, SUMO-1 (Weger *et al.*, 2003), and both endogenous h-topors and overexpressed h-topors-GFP fusion protein are mainly distributed in promyelocytic leukemia-associated protein (PML) nuclear bodies in a PML protein-dependent fashion (Rasheed *et al.*, 2002). The carboxyl-terminal region of h-topors is required for such punctate nuclear localization (Rasheed *et al.*, 2002). In addition, the amino-terminal region of h-topors, containing the RING zinc-finger motif and LZ region, has been shown to bind to DNA in a sequence-specific as well as Zn^{2+}-dependent manner (Chu *et al.*, 2001). Since h-topors enhances the expression of a Rep78/68-dependent AAV-2 gene in the absence of helper virus, h-topors might be a transcriptional regulator (Weger *et al.*, 2002).

Although h-topors interacts with p53 as revealed by yeast two-hybrid assay, the role of h-topors in regulating the function of p53 remains to be clarified (Zhou *et al.*, 1999; Weger *et al.*, 2002). Several lines of evidence suggest that h-topors might be an important regulator in cell proliferation. Relocalization of topors in cells exposed to the Top1-targeting drug camptothecin (CPT) or the transcription inhibitor 5,6-dichloro-1-β-D-ribofuranolsylbenzimidazole (DRB) suggests its involvement in mediating the DNA damage response induced by CPT or DRB, which have been shown to cause an accumulation of p53 (Klibanov *et al.*, 2001; Rasheed *et al.*, 2002). h-topors interacts with AAV-2 Rep78, which has been proved to be an effective repressor of the adenovirus in the process of tumor generation (Schlehofer, 1994). Intriguingly, the region of h-topors required for interaction with AAV-2 Rep78/68 overlaps with that for p53 binding, as revealed by yeast two-hybrid analysis (Batchu *et al.*, 1999; Weger *et al.*, 2002). In addition, h-topors maps to chromosome 9p21, a locus containing candidate tumor suppressor gene(s) associated with the loss of heterozygosity in 86% of small cell lung cancers (Chu *et al.*, 2001). These observations prompted us to examine the functional role of topors in the regulation of p53. In the present study, we describe a physical and functional interaction between mouse topors and p53 in mammalian cultured cells. Our results strongly suggest that topors acts as a coactivator of p53 in response to DNA damage.

Results

Identification of a murine counterpart of topors

To identify proteins that interact with the Polycomb group (PcG) protein Mph2 (Yamaki *et al.*, 2002), we employed yeast-based two-hybrid screening using a cDNA library derived from mouse embryo and bait derived from full-length Mph2. We isolated two identical 1.2-kb cDNA fragments encoding a polypeptide highly homologous to the carboxyl-terminal half of h-topors. By conventional cDNA screening of a mouse brain cDNA library and database screening, two overlapping clones, a 3.5-kb fragment lacking the amino-terminal region and a mouse EST clone lacking the carboxyl-terminal region, were isolated. The nucleotide sequences of both clones were determined, and the combined nucleotide sequences revealed the longest open reading frame (ORF) of 1033 amino-acid residues with 86% overall identity to h-topors (DDBJ accession number: AB104865). In the amino-terminal region, a RING family zinc-finger domain and an LZ region exhibited 100 and 98% homology to h-topors, respectively (red letters and open blue box in Figure 1a, respectively). The p53-binding domains of h-topors were previously shown to be separated into two blocks based on yeast two-hybrid interactions (underlined in Figure 1a) (Zhou *et al.*, 1999; Weger *et al.*, 2002). A bipartite NLS was present in the amino-terminal block of the p53-binding domains (blue letters in Figure 1a). A cluster of residues including the two p53-binding subdomains and an intermediate region exhibited 90% identity with h-topors (Figure 1b). Because of the extensive similarity to h-topors, this newly isolated cDNA was identified as a murine counterpart of the *h-topors* gene. The mouse *topors* gene was mapped to a 40 Mb region of mouse chromosome 4 by BLAST analysis of the mouse genome (40017898–40007704 bp; Ensemble Mouse Genome Browser), a region syntenic to human chromosome 9p21. This chromosomal localization is in agreement with a previous report in which human *topors* was mapped to the chromosome 9p21 region (Chu *et al.*, 2001).

h-topors has been shown to associate with PML nuclear bodies in exponentially growing HeLa cells (Rasheed *et al.*, 2002). To examine the subcellular localization of mouse topors in mammalian cultured cells, we constructed an expression vector encoding myc-epitope-tagged topors (myc-topors) and confirmed its expression by *in vitro* transcription/translation experiments as well as transient transfection into COS-7 cells (Figure 1c and d). Consistent with the previous observation, myc-topors migrated more slowly (195 kDa) than predicted based on the calculated molecular mass, which has been suggested to be due to the phosphorylation of serine residues in the RS domain (Haluska *et al.*, 1999). The subcellular localization of myc-topors was also examined in U2-OS cells by transient overexpression. In interphase nuclei of morphologically intact transfectants, the myc-topors protein was always localized in the nuclei. Two types of transfectants were reproducibly observed. One type exhibited a fine speckled distribution to form 10–20 foci and the other type showed larger, closely spaced dots with much stronger fluorescence in the nucleoplasm but excluded from the nucleolus (data not shown). These findings were identical to those of Haluska *et al.* (1999), who described the subcellular localization of a GFP fusion with h-topors in HeLa cells.

topors interacts with p53 and enhances p53-dependent transcription in mammalian cultured cells

The putative p53-binding domains revealed by yeast two-hybrid interaction (Zhou *et al.*, 1999; Weger *et al.*,

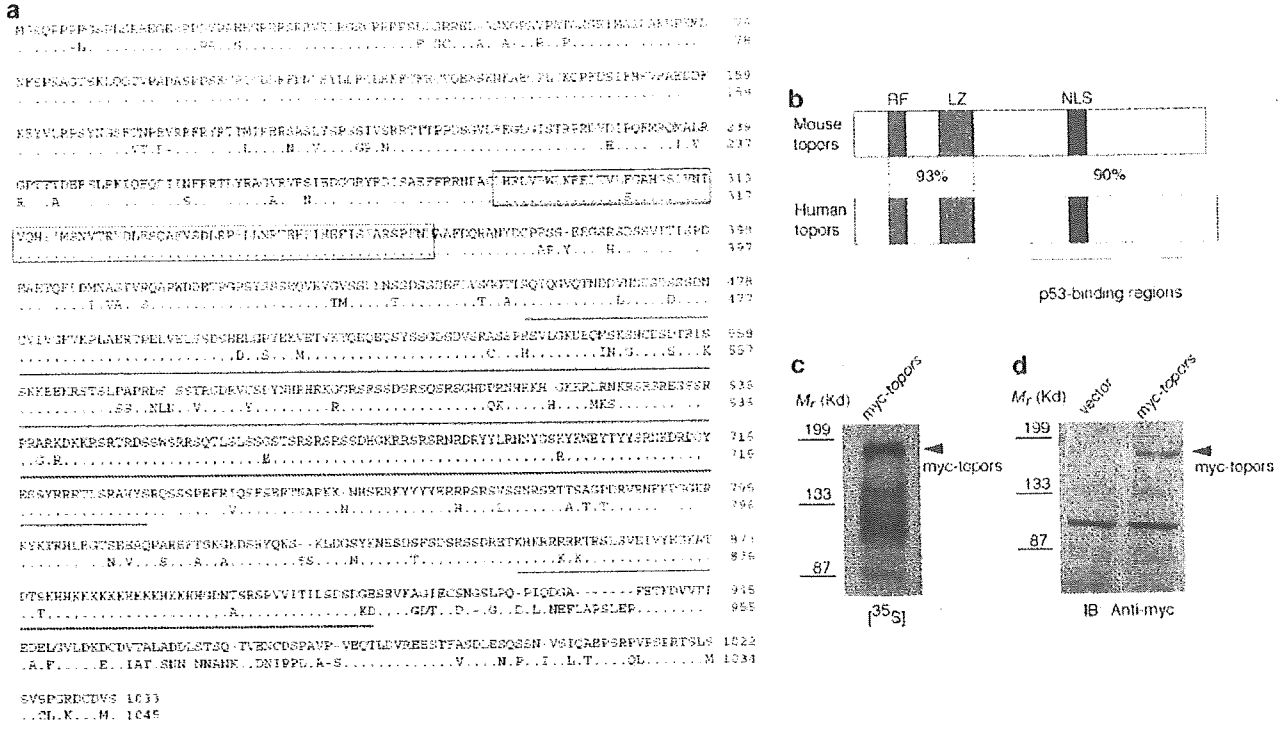

Figure 1 Amino-acid sequence, putative domain structure and expression of murine topors protein. **(a)** The deduced amino-acid sequence of mouse topors protein along with the sequence of the human counterpart. The sequences of mouse (top) and human (bottom) topors were aligned to provide the highest homology. Identical amino-acid residues are shown as dots in the human sequence; gaps are indicated by bars. Amino-acid residues in the putative RING finger motif and bipartite NLS are shown in red and blue letters, respectively. The region of the putative LZ structure is boxed with the hydrophobic residues at the first position of the heptad repeat shown in green letters. Two separate regions encoding putative p53-binding domains are underlined in red (see text). **(b)** Schematic representation of homologous domain structure shared between mouse and human topors. The RING finger motif (RF), LZ and bipartite NLS are indicated by red, green and blue boxes, respectively. Identical amino acids in each region are shown. **(c)** The myc-*topors* gene product generated by *in vitro* transcription/translation and analysed as described in Materials and methods. Relative molecular weight is indicated. **(d)** The myc-topors protein transiently overexpressed in COS-7 cells. Whole-cell lysates prepared from COS-7 cells transfected with either empty pcDNA3 (Vector, left) or pcDNA3-myc-*topors* (myc-*topors*, right) were subjected to immunoblotting analysis using the anti-myc monoclonal antibody

2002) are highly conserved between human and mouse topors (Figure 1a and b). This prompted us to examine whether myc-topors could interact with p53 in mammalian cultured cells. COS-7 cells were transiently transfected with myc-topors, and whole-cell extracts of the transfectants were subjected to immunoprecipitation with anti-p53 or normal mouse serum (NMS). As shown in Figure 2a, the anti-p53, but not the NMS, immunoprecipitates contained significant amounts of myc-topors, indicating that overexpressed myc-topors could associate with endogenous p53. This finding is consistent with the previous yeast two-hybrid studies demonstrating topors–p53 interaction (Zhou *et al.*, 1999; Weger *et al.*, 2002). We next addressed whether the physical interaction of topors with p53 might affect the function of p53. To this end, we examined the effects of overexpressed myc-topors on the p53-dependent transcription of *Bax*, *p21^{Waf1}* and *MDM2* promoters using luciferase assays in transiently transfected p53-deficient SAOS-2 and H1299 cells (Barak *et al.*, 1993; el-Deiry *et al.*, 1993; Miyashita and Reed, 1995). As shown in Figure 2b, the overexpression of myc-topors in SAOS-2 cells significantly enhanced p53-dependent transcription of the *Bax* and *MDM2* promoters in a dose-dependent manner. While myc-topors enhanced the p53-dependent activity of the *p21^{Waf1}* promoter in SAOS-2 cells, this effect did not achieve statistical significance (Figure 2b, middle panel). Similar results were obtained in H1299 cells, except that its effect on all three p53-responsive promoters was statistically significant as compared with p53 alone (Figure 2c). Under our experimental conditions, myc-topors alone had no effects on the *Bax*, *p21^{Waf1}* or *MDM2* promoter activity. We further studied whether the overexpression of topors influenced the expression of endogenous p53-regulated transcripts by quantitative real-time RT–PCR analysis of human *p21^{Waf1}* mRNA levels. As shown in Figure 2d and e, forced expression of topors enhanced the transcription of the p53 downstream gene *p21^{Waf1}* in both human small cell lung cancer SBC3 cells and U2-OS cells. Taken together, the results indicate that overexpression of topors enhances the sequence-specific transcriptional activity of p53 in a p53-dependent manner.

topors suppresses cell growth in a p53-dependent manner

These observations prompted us to investigate further whether the overexpression of myc-topors influences the growth suppression mediated by p53. For this purpose, we performed a colony formation assay using H1299 cells (lacking endogenous p53) and U2-OS cells containing the wild-type *p53* allele. The overexpression of myc-topors did not affect colony number in H1299 cells, while the colony number was significantly reduced in a dose-dependent manner in U2-OS cells (Figure 3a and b). The forced expression of p53 significantly reduced the colony number in H1299 cells, and this p53-dependent reduction was further intensified by cotransfection of pcDNA3-myc-*topors* (Figure 3a). Thus, the overexpression of topors appears to enhance the p53-dependent growth suppression of tumor cells.

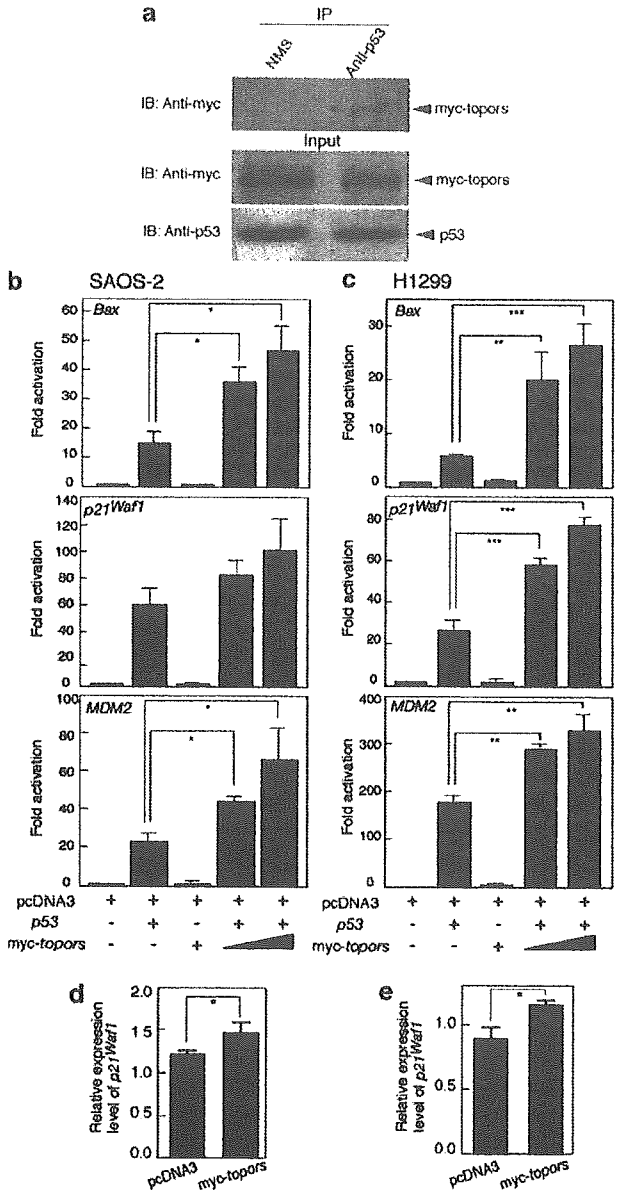

In different systems, p53 can induce apoptosis or cause cell cycle arrest (Ko and Prives, 1996; Vogelstein *et al*., 2000). Because topors was able to enhance p53-dependent growth suppression, we next examined whether topors-dependent growth suppression involves apoptosis. The number of apoptotic cells exhibiting nuclear condensation and fragmentation was counted 48 h after transfection with either pcDNA3-myc-*topors* or pEGFP (Figure 3c-I–III). The number of apoptotic cells increased significantly among U2-OS cells overexpressing myc-topors compared to pEGFP transfectants (Figure 3c-IV). Thus, the growth suppression resulting from overexpression of topors may result in part from induction of apoptosis.

Since p53 activation is known to cause not only apoptosis but also cell cycle arrest, we next examined the impact of overexpressed myc-topors on cell cycle progression. For this purpose, we established stable cell lines overexpressing myc-topors. U2-OS cells were transfected with pcDNA3-myc-*topors*, and G418-resistant clones were individually isolated and screened for myc-topors expression by immunofluorescent staining. Two cell lines out of 200 clones screened were found to express myc-topors (*topors* sta-1 and *topors* sta-2), and *topors* sta-1 expressed myc-topors at a higher level than *topors* sta-2 (Figure 4a). In both of the stable transfectants, myc-topors exhibited a speckled nuclear distribution to form 10–20 foci (Figure 4b), as did endogenous mouse topors in NIH 3T3 fibroblasts (data not shown) and as reported for endogenous human topors (Rasheed *et al*., 2002). *topors* sta-1 and *topors* sta-2 cells displayed a significantly slower growth rate

Figure 2 topors associates with p53 and activates p53-dependent transcription. (**a**) Association of transiently overexpressed myc-topors with endogenous p53 is shown by immunoprecipitation and subsequent immunoblotting analysis. (top) Whole-cell extract of COS-7 cells transfected with pcDNA3-myc-*topors* was subjected to immunoprecipitation with either NMS (left) or anti-p53 monoclonal antibodies (right) followed by immunoblotting with anti-myc monoclonal antibody. (middle and bottom) Unfractionated whole-cell extract of COS-7 cells transfected with myc-*topors* was subjected to immunoblotting using anti-myc monoclonal antibody (middle) or anti-p53 monoclonal antibody (bottom). (**b**, **c**) p53-deficient SAOS-2 (**b**) and H1299 (**c**) cells were transiently cotransfected with the expression plasmid for p53 along with luciferase reporter constructs containing the *Bax* (top), $p21^{Waf1}$ (middle) or *MDM2* (bottom) promoters in the presence or absence of increasing amounts of transfected pcDNA3-myc-*topors*. Transfection efficiency was standardized against *Renilla* luciferase. The average relative luciferase activities in triplicate experiments are represented as bars. Results are shown as fold induction of the luciferase activity compared with cells transfected with pcDNA3. Data shown are representative of two or three independent experiments with similar results. The significance of the differences was evaluated by Student's *t*-test (***$P<0.001$; **$P<0.01$; *$P<0.05$). (**d**, **e**) The expression of $p21^{Waf1}$ is upregulated by overexpression of myc-topors in small cell lung cancer cell SBC3 (**d**) and U2-OS cells (**e**). The expression of human $p21^{Waf1}$ was determined by quantitative real-time RT–PCR analysis as described in Materials and methods. Relative expression levels of $p21^{Waf1}$ were normalized to the levels of *β-actin* mRNA. The data shown are representative of two independent experiments with similar results. The significance of the differences was evaluated by Student's *t*-test (*$P<0.05$)

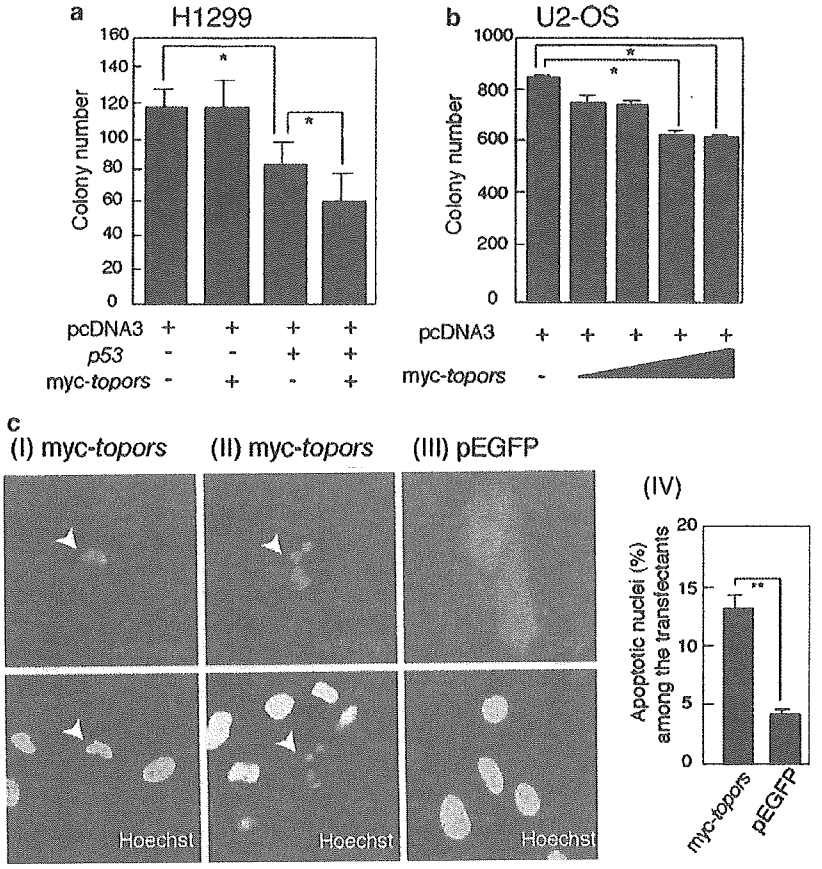

Figure 3 Enhancement of p53-dependent growth suppression and induction of apoptosis by the overexpression of topors. (**a**) The reduction in colony number by the transient overexpression of p53 is significantly enhanced by myc-topors in p53-deficient H1299 cells. (**b**) Increasing amounts of transfected myc-topors correlate with the reduction in colony number of U2-OS cells containing wild-type p53. Bars show the average numbers of colonies in triplicate experiments. The data shown are representative of three independent experiments with similar results. The significance of differences was evaluated by Student's *t*-test ($*P<0.05$). (**c**) Overexpression of myc-topors in U2-OS cells results in an increase in the number of apoptotic cells. U2-OS cells were transfected with either pcDNA3-myc-*topors* or pEGFP and transfected cells were identified by immunofluorescence staining with anti-myc monoclonal antibody or GFP expression, respectively (upper panels). Nuclear morphology was analysed after counterstaining with 1 μM Hoechst (lower panels). Cells overexpressing myc-topors frequently exhibit condensation (I) or fragmentation (II) of the nuclei, while GFP expression shows normal morphology (III). The percentages of apoptotic cells among >200 myc-topors- or GFP-positive cells were determined (IV). Values represent the means of three independent experiments. The significance of the differences was evaluated by Student's *t*-test ($**P<0.01$)

compared with the parental U2-OS cells and U2-OS cells transfected with empty vector (V-1) (Figure 4c). Of note, *topors* sta-1 cells grew more slowly than *topors* sta-2 cells, suggesting that the growth rate correlated inversely with the level of myc-topors expression in the respective cell lines. Next, asynchronous cultures of these transfectants and the parental cells were collected at 48 h after culture and their cell cycle distribution was analysed by flow cytometry. As shown in Figure 4d (cisplatin (−)) and e, *topors* sta-1 and *topors* sta-2 cells displayed a significant increase in the percentage of cells in G1 phase as compared with U2-OS and V-1 cells. A slight but reproducible increase in the sub-G1 fraction was seen exclusively in *topors* sta-1 cells (even without cisplatin treatment; see below), suggesting the constitutive occurrence of apoptosis in the *topors* sta-1 transfectants (Figure 4d and f (cisplatin (−))). The severe growth retardation of U2-OS cells stably expressing myc-topors might therefore result from both a prolonged G1 phase and a subtle induction of apoptosis. Comparison of the *topors* sta-1 and *topors* sta-2 results suggests that overexpression of topors can result in growth arrest and/or apoptosis depending on the degree of topors expression and the particular cellular context.

Stabilization of p53 by overexpression of topors

To determine whether the growth retardation produced by the stable overexpression of myc-topors was linked to the activation of p53, we next examined the expression of p53 and its response gene product, $p21^{Waf1}$ (Harper *et al.*, 1993), in permanent transfectants. p53 was more abundantly expressed in both *topors* sta-1 and *topors* sta-2 stable transfectants than in control cell lines and the expression of $p21^{Waf1}$ was greater in both topors

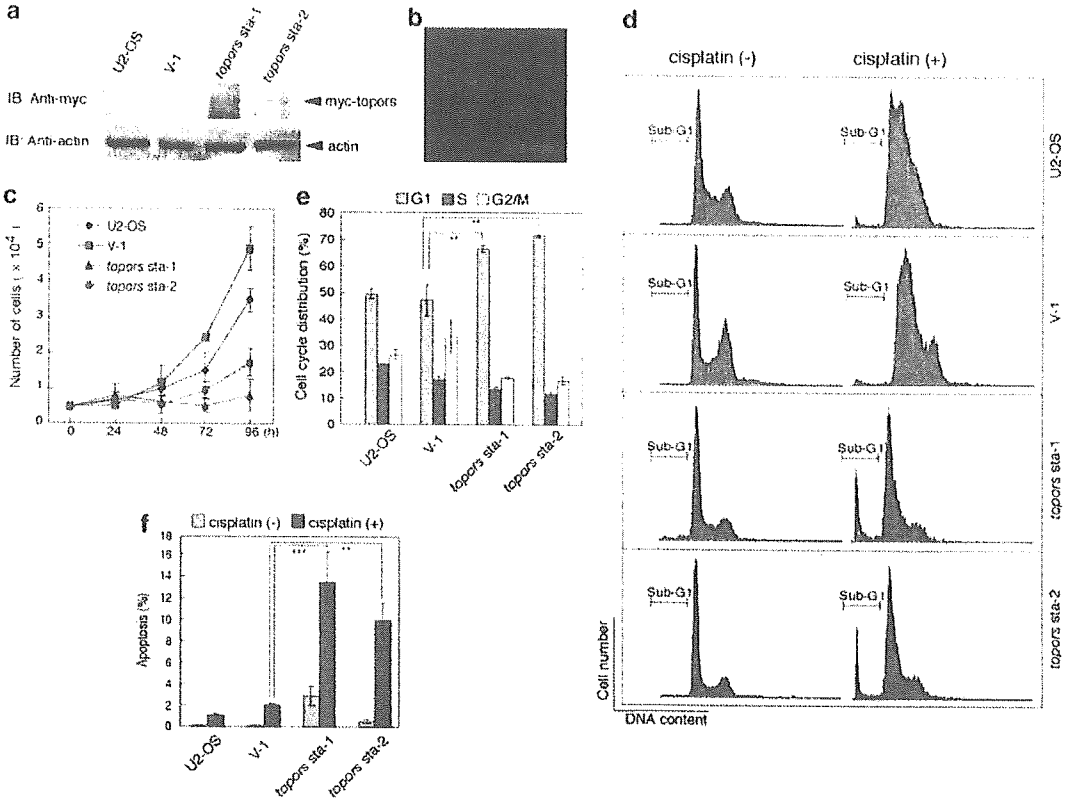

Figure 4 Cell cycle arrest and DNA damage-mediated apoptosis in U2-OS cells stably overexpressing myc-topors. (**a**) The expression of myc-topors in parental U2-OS cells and stable empty pcDNA3 vector (V-1) and pcDNA3-myc-*topors* (*topors* sta-1 and sta-2) transfectants as revealed by immunoblotting analysis using a polyclonal anti-myc antibody. The expression of actin is shown below as a loading control. (**b**) The expression pattern of myc-topors in *topors* sta-1 cell nuclei as revealed by immunofluorescent staining with anti-myc monoclonal antibody. (**c**) Growth rates of the indicated cells. The indicated cells were seeded at a density of 0.5×10^4 cells/well (12-well plate) and cell numbers were determined 1, 2, 3 and 4 days later. Average cell numbers at each time point determined in triplicate experiments are shown; standard deviations are shown in parentheses. Representative results of three independent experiments are shown. (**d**) Exponentially growing stable transfectants and control cells treated without or with cisplatin were stained with propidium iodide (PI) and subjected to FACS analysis. Representative FACS profiles of each cell line without (left) or with (right) cisplatin treatment are shown. Sub-G1 fractions are indicated. (**e**) Cell cycle profiles of exponentially growing U2-OS-derived cells as revealed by FACS analysis are shown by histograms. (**f**) Frequency of apoptotic cells among cells treated without (−) and with (+) cisplatin is shown by histograms. Values are the average percentages from triplicate experiments, and standard deviations are shown in parentheses. The experiments were repeated three times with essentially similar results. The significance of differences was evaluated by Student's *t*-test (***$P<0.001$; **$P<0.01$)

stable transfectants than in controls (Figure 5a). The increased level of $p21^{Waf1}$ protein correlated with the topors-enhanced expression of $p21^{Waf1}$ mRNA in small cell lung cancer cells and U2-OS cells shown above (Figure 2d and e). Importantly, the upregulation of p53 and $p21^{Waf1}$ proteins in *topors* sta-1 was stronger than in *topors* sta-2, consistent with the relative expression level of ectopic myc-topors and the severity of the growth phenotypes in the two cell lines. The levels of expression of the p53 protein could also be increased by transient overexpression of myc-topors in U2-OS cells and p53-deficient large cell lung carcinoma H1299 cells, which were cotransfected with both FLAG-tagged *p53* and myc-*topors* (Figure 5c and d). Since the level of *p53* transcript was not significantly different in either of the permanent transfectants compared to controls (Figure 5b), it is likely that the increase in the amount of p53 protein was due to its stabilization. To investigate whether an increased protein half-life contributed to the elevated levels of p53 observed, we then determined the decay rate of p53 protein without and with topors overexpression. At 24 h after culture of the empty vector stable cells (V-1) and *topors* sta-2 cells, or 24 h post-transient transfection of p53-deficient human large cell lung carcinoma H1299 cells with FLAG-*p53* along with either pcDNA3 or pcDNA3-myc-*topors*, cells were treated with the protein synthesis inhibitor cycloheximide at a final concentration of 100 μg/ml for 0, 2, 4 and 6 h. The expression of p53 was then examined by immunoblotting for each time point and normalized by reference to the level of actin in each sample. As shown in Figure 5e, the p53 protein possessed a greater half-life in *topors* sta-2 cells compared with V-1 vector-transfected U2-OS cells. Similarly, the half-life of p53 was prolonged in the presence of topors compared to that of p53 cotransfected with pcDNA3 vector in p53-deficient

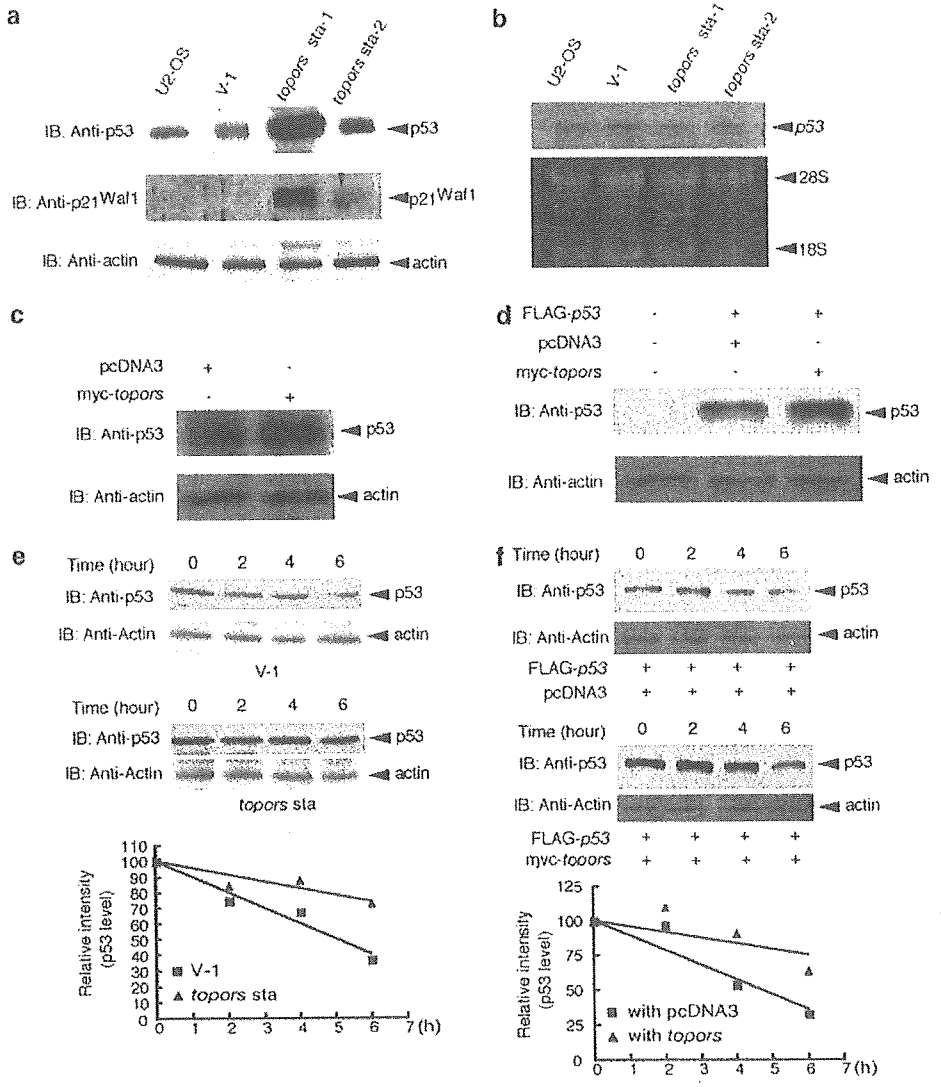

Figure 5 Stabilization of p53 protein by overexpression of myc-topors. (**a**) The expressions of p53 and $p21^{Waf1}$ in parental U2-OS cells and stable transfectants of pcDNA3 vector (V-1) and pcDNA3-myc-*topors* (*topors* sta-1 and sta-2) as revealed by immunoblotting analysis. The expression of actin is shown as a loading control. (**b**) The expression of *p53* transcript in each cell line as revealed by RNA blot analysis (upper panel). Ethidium bromide staining of 28S and 18S ribosomal RNA is shown as a loading control (lower panel). (**c**) The expression of p53 in U2-OS cells after transfection with pcDNA3 or pcDNA3-myc-*topors*. The expression of actin is shown as a loading control. (**d**) The expression of p53 in H1299 cells after transfection without or with FLAG-*p53* in the presence of pcDNA3 or pcDNA3-myc-*topors*. The expression of actin is shown as a loading control. (**e, f**) Increase in the half-life of p53 by topors. At 24 h after culture of pcDNA3 stable cells (V-1) and *topors* sta-2 cells (**e**), or at 24 h after transient transfection of p53-deficient H1299 cells (**f**) with expression plasmid of FLAG-*p53* along with pcDNA3 or pcDNA3-myc-*topors*, cycloheximide was added to the culture medium and the cells were extracted at the indicated time points. Whole-cell lysates were subjected to immunoblotting. The relative intensities of p53 were quantified by densitometric scanning, which normalized to actin, and are represented graphically

H1299 cells (Figure 5f). Taken together, these data suggest that expression of topors increases p53 levels by stabilizing p53 protein and thereby enhancing its ability to limit cell growth.

topors expression is induced by DNA damage

Our finding that transient or stable transfection of topors upregulates p53 levels suggests that topors could be a rate-limiting factor in the regulation of p53 function. If this is the case, a quantitative alteration of topors expression in a given cell could affect its apoptotic response to genotoxic reagents. To address this possibility, exponentially growing U2-OS cells or stable transfectants were treated with 20 μM cisplatin for 24 h, and the cells were then subjected to the cell cycle analysis. Following cisplatin treatment, both *topors* sta-1 and *topors* sta-2 cells demonstrated significantly increased sub-G1 fractions compared to the control cells (Figure 4d and f). The fraction of apoptotic cells among the *topors* sta-1 and *topors* sta-2 transfectants reached 80–90% after 48 h of cisplatin

treatment, compared to only 30–40% in control cells (data not shown). Thus, the overexpression of topors enhances the apoptotic response of U2-OS cells to DNA damage.

This finding suggests that upregulation of endogenous topors might be involved in mediating p53-dependent cellular responses to stress stimuli. We thus examined the expression of endogenous *topors* after cisplatin treatment in U2-OS cells. *topors* expression was obviously upregulated 24 and 48 h after cisplatin treatment consistent with the expression of p53 protein (Figure 6a). The analysis was extended to primary MEFs and C-20 cells, a mouse cell line derived from colon carcinoma. In these cells before treatment, *topors* was constitutively expressed while p53 was barely detectable. The apoptotic response of MEFs and C-20 cells to 20 μM cisplatin was more prominent than that of U2-OS cells (Figure 6b and c; compare to Figure 4d). The expression of the *topors* gene and p53 protein was increased in MEFs and C-20 cells by cisplatin treatment as well (Figure 6b and c). Since topors is a topoisomerase I-binding protein, we further investigated whether the expression of *topors* is also induced after treatment by CPT, a potent antineoplastic inhibitor of topoisomerase I (Haluska *et al*., 1999). As shown in Figure 6d, when U2-OS cells and NIH 3T3 cells were treated with CPT at the concentration of 10 μM, the expression of *topors* increased more than twofold compared to cells without treatment. However, it is still possible that the upregulation of *topors* mRNA might be a consequence of p53 induced during DNA damage-induced apoptosis. To exclude this possibility, we examined *topors* expression after overexpression of p53 by transient transfection. The overexpression of p53 did not significantly affect *topors* transcript levels (Figure 6e). Taken together, the induction of *topors* by the genotoxic reagents provides a mechanism to facilitate the p53-mediated DNA damage-dependent apoptosis in tumor and primary cells.

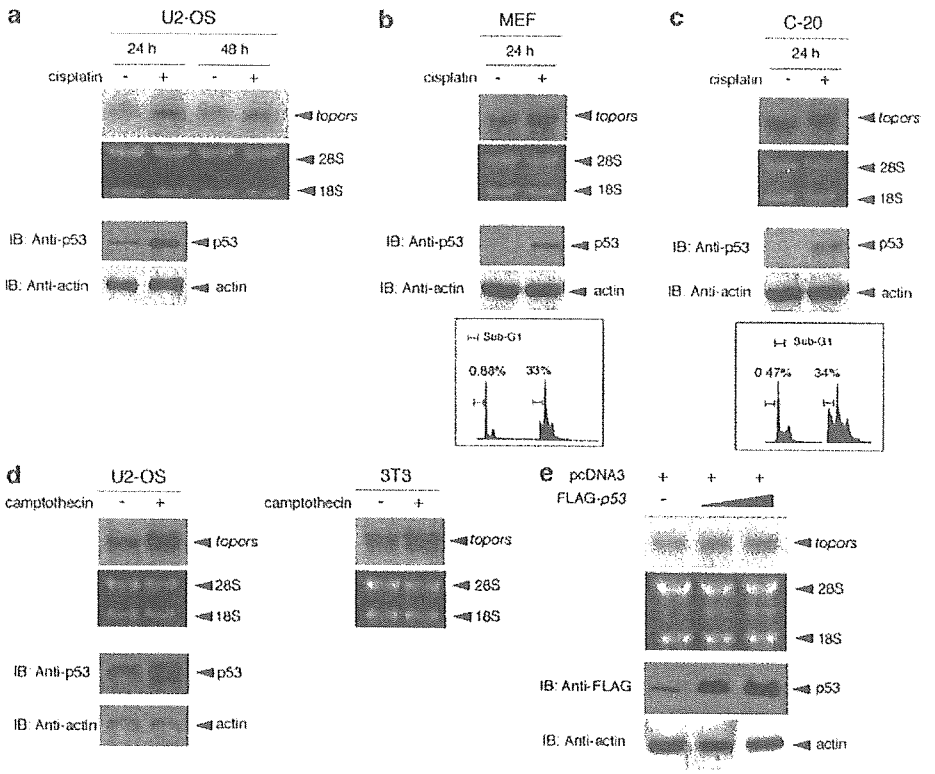

Figure 6 Induction of endogenous *topors* expression by DNA damage in human and mouse cell lines. (**a**) The expressions of *topors* and p53 are significantly induced in U2-OS cells in response to cisplatin treatment as revealed by RNA blot and immunoblotting analysis, respectively. (upper panels) *topors* transcripts detected as 4.0-kb bands (top) and ethidium bromide staining of 28S and 18S ribosomal as a loading control are shown (bottom). (lower panels) The expressions of p53 (top) and actin (lower) as a loading control are shown. (**b**, **c**) Induction of *topors* (upper panels), p53 expression (middle panels) and FACS analysis-based estimation of apoptosis (lower panels) by cisplatin treatment are also seen in primary MEFs (**b**) and murine colon carcinoma cells (C-20) (**c**). Percentages of cells in the sub-G1 fraction are shown in the lower panels. (**d**) The expressions of *topors* and p53 are significantly induced in U2-OS cells and NIH/3T3 cells in response to 12-h CPT treatment as revealed by Northern blot and immunoblotting, respectively. (upper panels) *topors* transcripts (top) and ethidium bromide staining of 28S and 18S ribosomal as a loading control are shown (bottom). (lower panel) The expressions of p53 (top) and actin (lower) as a loading control in U2-OS cells are shown. (**e**) The expression of *topors* is not affected by the transient overexpression of p53 in U2-OS cells. Increasing amounts of FLAG-*p53* documented by immunoblotting analysis (lower panels) do not significantly affect the expression of endogenous *topors* (upper panels). Ethidium bromide staining of 28S and 18S ribosomal RNA is shown as a loading control

Discussion

In the present study, we identify the mouse counterpart of human topors and document its involvement in p53-regulated cell growth control. Overexpressed topors associates with p53, activates p53-dependent transcription via the stabilization of p53 and, consequently, induces either cell cycle arrest or apoptosis in a dose-dependent manner. Therefore, our observations strongly implicate the topors protein as a novel coactivator of the p53 tumor suppressor protein.

We further show that expression of endogenous *topors*, as well as the p53 protein, is induced by DNA damage in tumor and primary cells. The present observations indicate that topors mediates p53-dependent cellular responses to some forms of DNA damage and, thus, could act as a tumor suppressor that activates p53. Interestingly, the human *topors* gene maps to chromosome 9p21 where the tumor suppressor genes associated with 86% of small cell lung carcinomas are suggested to reside and the above observations provide further evidence for the *topors* gene as a candidate tumor suppressor gene mapped to this region. Our preliminary studies have revealed that *topors* mRNA is expressed in all small cell lung cancer cell lines at levels similar to other tumor cell lines (L Lin and A Hata, unpublished data). Most recently, Oyanagi *et al.* (2004) revealed that the expression of *LUN* (*topors*) gene is downregulated in the development and metastases of lung cancer, suggesting that *LUN* might play important roles in inhibiting the oncogenesis of non-small cell lung cancer. The expression of topors protein in normal lung tissues and small cell lung cancers will require further future study.

The data clearly show that the overexpression of topors may cause either cell cycle arrest or apoptosis, and suggest that which occurs depends both on the topors level and the cellular context, although other variables require further exploration. There is a positive correlation between the amount of p53 protein and overexpressed topors in U2-OS cells in both transient and stable transfectants. Since it has repeatedly been reported that low levels of p53 expression are antiapoptotic while high levels promote apoptosis, high levels of topors could facilitate apoptosis due to the high level of p53 expression (Chen *et al.*, 1996; Lassus *et al.*, 1996). This phenomenon is further supported by another observation made in this study. We identified only two stable transfectants overexpressing myc-topors from 200 G418-resistant colonies and both exhibited a lower level of topors expression than that seen in the transiently transfected cells. This implies that only U2-OS cells overexpressing permissive amounts of exogenous topors might be allowed to survive by escaping apoptotic outbursts and instead exhibiting G1 cell cycle arrest, which is correlated with the induction of the downstream gene of p53, $p21^{Waf1}$. Interestingly, slight but significant apoptotic outbursts coincide with G1 arrest in *topors* sta-1, but not sta-2, cells. Slightly higher expression levels of myc-topors and, consequently, p53 in *topors* sta-1 cells than in sta-2 cells may be the cause for this phenotypical difference.

Our findings demonstrate that the expression level of topors protein may be a rate-limiting factor in the regulation of p53 activity. While this manuscript was in preparation, Saleem *et al.* (2004) also reported that transient expression of h-topors showed antiproliferative activity and was associated with G0/G1 cell cycle arrest in HeLa cells. Our results additionally show that overexpression of topors could activate the expression of p53 and induce either cell cycle arrest or apoptotic response.

In this study, we show that endogenous topors is significantly upregulated by the genotoxic reagents at the level of transcription in tumor and primary cells. A previous study has suggested that post-translational regulation of topors by DNA damage may also be involved (Rasheed *et al.*, 2002). In that study, overexpressed GFP-topors fusion protein immediately relocalized from PML nuclear bodies to the nucleoplasm in cells exposed to CPT or DRB. Since DRB exposure has also been shown to induce the accumulation of diffuse p53 in the nucleoplasm, it is possible that the relocalization of topors into the nucleoplasm might allow its association with and subsequent stabilization of p53 (Klibanov *et al.*, 2001).

The stability of the tumor suppressor p53 is crucial for its function to induce cell cycle arrest and/or apoptosis as a consequence of its ability to bind to specific DNA sequences and activate the transcription of adjacent genes (Vogelstein *et al.*, 2000). Overexpression of topors increased the stability of p53 and correspondingly enhanced the p53-dependent transcriptional activities. topors contains a RING finger motif, a domain that has been implicated in protein–DNA and protein–protein interactions, E2-dependent ubiquitination and SUMO conjugation (Kahyo *et al.*, 2001; Matthews and Sunde, 2002). Indeed, topors proteins have been recently shown to possess evolutionarily conserved E3 ubiquitin ligase activity. A *Drosophila* topors was shown to mediate Hairy polyubiquitination, resulting in Hairy, but not Dmp53 or topoisomerase I (dTopoI), degradation (Secombe and Parkhurst, 2004). Human GFP-topors fusion protein was shown to function as an E3 ligase for p53, albeit to a lesser degree than MDM2 (Rajendra *et al.*, 2004). Therefore, topors could affect the stability of p53 via covalent modification of p53 by ubiquitin isopeptide. This observation, however, is not necessarily consistent with our and others' previous observations suggesting topors as a likely tumor suppressor protein since polyubiquitination of p53 mediated by GFP-topors induces proteasome-dependent downregulation of p53 in U2-OS cells (Chu *et al.*, 2001; Rajendra *et al.*, 2004; Saleem *et al.*, 2004). This implies that regulation of p53 by topors may involve not only ubiquitination but also some other molecular mechanism.

Recently, the activity of p53 has been reported to be positively regulated by SUMO conjugation, which is mediated, at least in part, by another RING finger protein, PIAS (Gostissa *et al.*, 1999; Rodriguez *et al.*, 1999; Kahyo *et al.*, 2001). Sequence similarity between

two regions of topors and human PIASx protein, the RING domains and putative SUMO-1 interaction motifs suggests the possibility that topors may function as a SUMO E3 ligase (Weger *et al.*, 2003). Indeed, h-topors and several components of SUMO-conjugating systems have been isolated together as interacting proteins with Mx1, an interferon-inducible GTPase that is associated with PML nuclear bodies (Engelhardt *et al.*, 2001), which include p53, pRb, DAXX and CBP (Mann and Miller, 2004). Thus, topors may contribute to p53 stabilization or activation via SUMO conjugation processes.

The molecular mechanisms underlying the stabilization and/or activation of p53 by topors may also involve protein–protein interactions. AAV-2 Rep78/68 has been shown to possess a tumor suppressor property and to bind physically to p53 to prevent the adenovirus-mediated degradation of p53 (Batchu *et al.*, 1999). Since topors is capable of interacting not only with p53, but also with Rep78/68, topors may cooperate with Rep78/68 to stabilize p53. It is possible that endogenous cellular regulators of p53 may function in ways analogous to these viral products and cooperate with topors to stabilize p53. These possibilities are not necessarily mutually exclusive. It will be essential to address experimentally the possible catalytic activities of topors.

Materials and methods

Isolation and preparation of an expression vector for a full-length cDNA of topors

Yeast two-hybrid screening was performed to isolate the cDNAs for Mph2-binding proteins from a cDNA library derived from E11.0 mouse embryo as described previously, and 177 independent clones were found to be positive for β-galactosidase activities as examined by filter assay (Vojtek *et al.*, 1993; Kingma and Osheroff, 1998; Yamaki *et al.*, 2002). The nucleotide sequences of the positive cDNA clones were determined. Two clones contained 1.2-kb cDNA fragments that were highly homologous to *h-topors* (Haluska *et al.*, 1999). To isolate a full-length *topors* cDNA, a radiolabeled 1.2-kb cDNA fragment was used as a probe to screen the mouse brain cDNA library. After three rounds of hybridization, six positive clones were obtained and their nucleotide sequences were determined. The longest cDNA, containing a 3.5-kb insert, turned out to encode from the RING finger motif to the stop codon, but lacked a putative *topors* initiation codon. By searching public databases of mouse ESTs, we found a cDNA clone (MNCb-6014) that overlapped with the 3.5-kb cDNA clone. MNCb-6014, which was kindly provided by Dr Katsuyuki Hashimoto (Division of Genetic Resources, National Institute of Infectious Diseases, Japan), contained a *topors* initiation codon, but instead lacked the carboxyl-terminal region. To generate an expression vector encoding a full-length *topors*, the 5′-region of MNCb-6014 was amplified with primers 5′-CGTCGACAAGCTTATGGGGTCGCAGC CGCC-3′ (the *SalI*/*HindIII* restriction sites are underlined) and 5′-CAGAAGACAGTTCAACAAGTTCCGGGGTCC-3′ using the MNCb-6014 cDNA clone as a template. The PCR product was digested with *SalI* and *SphI* and subcloned into the identical restriction sites of the above-mentioned plasmid containing the 3.5-kb insert to produce a full-length cDNA for *topors* (pBluscript-M-*topors*). The pBluscript-M-*topors* was digested with *HindIII* and *NotI* and introduced into the identical restriction sites of pcDNA3-myc (Invitrogen, Carlsbad, CA, USA) to generate an expression vector for myc-tagged topors (pcDNA3-myc-*topors*).

In vitro *transcription/translation of the topors gene product*

The topors protein was generated from the pcDNA3-myc-*topors* vector using the T7-TNT Quick-Coupled Transcription–Translation system (Promega, Madison, WI, USA) in the presence of [^{35}S]methionine (Amersham Biosciences Inc., Piscataway, NJ, USA) according to the manufacturer's instructions. The quality of the synthesized protein was verified by electrophoresis though an 8% SDS–polyacrylamide gel and autoradiography.

Cell culture and transfection

Human osteosarcoma cell lines U2-OS and SAOS-2, COS-7, NIH/3T3 and primary MEFs were maintained in DMEM supplemented with 10% FBS and antibiotics. Human large cell lung carcinoma H1299 cells and human small cell lung cancer SBC3 cells were grown in RPMI-1640 medium supplemented with 10% FBS and antibiotics. All cells were cultured at 37°C in a water-saturated atmosphere of 5% CO_2 in air. COS-7 and U2-OS cells contain wild-type p53, while SAOS-2 and H1299 cells are deficient in p53 expression. For transfection, U2-OS cells were transfected by either the calcium phosphate co-precipitation method or Lipofectamine 2000 transfection reagent (Invitrogen, Grand Island, NY, USA) in accordance with the manufacturer's specifications. COS-7 cells were transfected with the FuGENE6 transfection reagent (Roche Molecular Biochemicals, Indianapolis, IN, USA). H1299 and SAOS-2 cells were transfected with the LipofectAMINE Plus transfection kit (Invitrogen, Grand Island, NY, USA) according to the manufacturer's protocol. To obtain stable transfectants, either pcDNA3 or pcDNA3-myc-*topors* was introduced into the exponentially growing U2-OS cells by the calcium phosphate co-precipitation method. At 48 h post-transfection, the cells were transferred to fresh medium containing G418 at a final concentration of 800 μg/ml. At 1 week after selection, drug-resistant colonies were isolated and the expression of myc-topors was examined by immunofluorescence staining as described below. As a control, a stable cell line of the pcDNA3 vector was established.

Immunoprecipitation and immunoblotting

Transfected cells were washed in ice-cold phosphate-buffered saline (PBS), lysed in lysis buffer (25 mM Tris-Cl, pH 7.5, 137 mM NaCl, 2.7 mM KCl, 1% Triton X-100 and 1 mM PMSF) and the extracts were sonicated briefly and centrifuged at 800*g* for 5 min to remove insoluble materials. The protein concentrations were determined by the Bradford protein assay (Bio-Rad, Hercules, CA, USA) using BSA as a standard. For immunoprecipitation, the cell lysates prepared from COS-7 cells transfected with pcDNA3-myc-*topors* were precleared using protein G-Sepharose beads at 4°C for 30 min under gentle rotation, and then incubated with either NMS or antibodies against p53 (DO-1, Oncogene Research Products, Cambridge, MA, USA and Pab1801, Santa Cruz Biotechnology Inc., Santa Cruz, CA, USA) at 4°C for 2 h. The immune complexes were then recovered with protein G-Sepharose beads. The immunoprecipitates or supernatants were subjected to SDS–polyacrylamide gel electrophoresis and electrophoretically transferred onto Immobilon P membranes (Millipore

Corp., Bedford, MA, USA). The membranes were blocked with TBS containing 0.1% Tween 20 and 5% nonfat dry milk, probed with antibodies against c-myc epitope (562, Medical and Biological Laboratories, Nagoya, Japan), p53 (DO-1, Oncogene Research Products, Cambridge, MA, USA), $p21^{Waf1}$ (H-164, Santa Cruz), β-actin (20-33, Sigma Chemical Co., St Louis, MO, USA) and FLAG (M2, Sigma Chemical Co., St Louis, MO, USA), and then incubated with horse radish peroxidase-conjugated goat anti-rabbit or anti-mouse secondary antibody (Santa Cruz Biotechnology Inc., Santa Cruz, CA, USA). Immunoreactive bands were visualized with an ECL Western blot detection kit (Amersham Biosciences Inc., Piscataway, NJ, USA).

Immunofluorescence and confocal microscopy

Transfected cells grown on coverslips were fixed with 3.7% formaldehyde for 30 min at room temperature, permeabilized with 0.2% Triton X-100 for 5 min at room temperature and then incubated with 3% BSA in PBS for 2 h to reduce nonspecific antibody binding. Immunostaining was performed by incubating cells with a monoclonal anti-myc antibody (9E10, diluted 1 : 10) for 1 h at room temperature in a humidified chamber, followed by incubation with fluorescein isothiocyanate (FITC)-conjugated goat anti-mouse IgG (diluted 1 : 250) for 1 h at room temperature. The coverslips were washed extensively with PBS, mounted with PermaFluor (Immunon, Pittsburgh, PA, USA) and the labeled cells were examined using a confocal laser scan microscope (LSM510; Carl Zeiss Co., Ltd, Jena, Germany).

Luciferase reporter assay

SAOS-2 or H1299 cells were seeded at a density of 5×10^4 cells/well in a 12-well tissue culture dish and then cotransfected with 100 ng of p53/p73-responsive luciferase reporter constructs carrying *Bax*, $p21^{Waf1}$ or *MDM2* promoter, 10 ng of pRL-TK and 25 ng of the p53 expression plasmid in either the presence or absence of increasing amounts of pcDNA3-myc-*topors* as described previously (Watanabe *et al*., 2002). The total amounts of DNA used in each transfection were kept constant (510 ng/transfection) using pcDNA3. Luciferase assays were performed 48 h post-transfection with a dual luciferase reporter assay system (Promega) according to the manufacturer's instructions.

Quantitative real-time RT–PCR analysis

Small cell lung cancer cell SBC3 and U2-OS cells were transfected with pcDNA3 or myc-*topors*. At 48 h after transfection, total RNA was extracted with the RNeasy Mini kit (Qiagen Inc., Valencia, CA, USA). Quantitative real-time RT–PCR was performed using the Brilliant SYBR Green QRT-PCR Master Mix Kit, 1-Step (Stratagene, La Jolla, CA, USA) and specific primers for human $p21^{Waf1}$ and human *β-actin*. Quantitative results of $p21^{Waf1}$ mRNA were normalized for the levels of *β-actin* mRNA. Specific primers for $p21^{Waf1}$ are as follows: 5′-ATGAAATTCACCCCCTTTCC-3′ (forward primer) and 5′-CCCTAGGCTGTGCTCACTTC-3′ (reverse primer).

Colony formation assay

U2-OS and H1299 cells were transfected with pcDNA3 or pcDNA3-myc-*topors* in the presence or absence of FLAG-*p53* (a kind gift from Dr Toshiharu Suzuki, University of Tokyo, Tokyo, Japan). After 48 h of culture, the cells were divided into new dishes and cultured for 2 weeks in the presence of 400 μg/ml of G418. The cell dishes were fixed, stained with Giemsa's solution (Merck KgaA, 54271, Darmstadt, Germany, Art. 1.09204) and the colonies were counted.

Analyses of cell cycle and apoptosis

After treating cells with or without cisplatin (Sigma Chemical Co., St Louis, MO, USA) at a final concentration of 20 μM for 24 h, both floating and adherent cells were collected by brief centrifugation, fixed in 70% (v/v) ethanol for more than 4 h at −20°C and stained with PI (Sigma Chemical Co., St Louis, MO, USA). To identify cells with sub-G1 DNA content, the fluorescence of the nuclei was measured by flow cytometry (FACScan, Becton Dickinson, Oxford, UK). At least 5×10^4 events were analysed with Cell Quest software. For the morphological assessment of fragmented nuclei, U2-OS cells grown on coverslips were transfected with either myc-*topors* or pEGFP-N3 (BD Biosciences, CA, USA). At 48 h post-transfection, the cells were fixed with 3.7% formaldehyde, permeabilized with 0.2% Triton X-100 and blocked with 3% BSA in PBS. myc-topors was visualized with 9E10 monoclonal antibody (diluted 1 : 10) followed by FITC-conjugated goat anti-mouse IgG (diluted 1 : 250). DNA was visualized by incubating the cells with 1 mM Hoechst 33258 dye. Cells showing apoptotic morphological changes were analysed under a Leica QFluoro confocal spectral microscope (Leica Microsystems Imaging Solutions Ltd, Cambridge, UK).

Protein half-life determination

At 24 h after culture of the pcDNA3 stable cells (V-1) and *topors* sta-2 cells, or at 24 h post-transfection of p53-deficient human H1299 cells with FLAG-*p53* in combination with either pcDNA3 or pcDNA3-myc-*topors*, cycloheximide (Sigma) was added to the cell culture medium at a final concentration of 100 μg/ml. Cells were collected at the indicated time points and whole-cell extracts were subjected to immunoblot analysis with anti-p53 antibody. Best-fit linear regression analysis of the data points was performed with Prism 4.0 software (GraphPad).

Northern blot analysis

U2-OS cells, MEFs, C-20 cells and NIH/3T3 cells were cultured in the presence of cisplatin (20 μM) for 24 or 48 h or CPT (10 μM) for 12 h. Total cellular RNA was isolated using the Isogen kit (Wako Pure Chemical Industries, Ltd, Osaka, Japan). RNA (10 μg) was denatured in formaldehyde-formamide, separated by electrophoresis in 1.5% agarose gels and transferred to Hybond™-N+ membranes (Amersham Biosciences, Tokyo, Japan). The resulting blots were individually hybridized with radiolabeled probes specific for *topors* and *p53* at 65°C for more than 10 h. The filters were washed twice with 2 × SSC (300 mM NaCl and 30 mM sodium citrate, pH 7.0)/0.1% *N*-lauroyl sarcosine at room temperature for 30 min, and then once with 1 × SSC/0.1% *N*-lauroyl sarcosine at 55°C for 30 min.

Statistical analysis

Statistical analyses were performed using the unpaired Student's *t*-test. The differences between two groups were considered to be statistically significant when $P < 0.05$.

Acknowledgements
We are grateful to Dr M Vidal and Dr O Tetsu for critical reading of the manuscript, Dr O Ohara for providing the mouse cDNA library, Dr T Oda for providing the pBTM116

vector, Ms Sanae Takeda, Dr Jie Liu and Dr Tomomi Kaneko for kind assistance and Dr T Akasaka for initial instructions on yeast two-hybrid screening. This project was supported by a grant-in-aid for Scientific Research on Priority Areas and for Scientific Research (B) and Special Coordination Funds for Promoting Science and Technology from the Ministry of Education, Culture, Sports, Science and Technology of the Japanese Government to HK and AN.

References

Barak Y, Juven T, Haffner R and Oren M. (1993). *EMBO J.*, **12**, 461–468.
Batchu RB, Shammas MA, Wang JY and Munshi NC. (1999). *Cancer Res.*, **59**, 3592–3595.
Chen X, Ko LJ, Jayaraman L and Prives C. (1996). *Genes Dev.*, **10**, 2438–2451.
Chu D, Kakazu N, Gorrin-Rivas MJ, Lu HP, Kawata M, Abe T, Ueda K and Adachi Y. (2001). *J. Biol. Chem.*, **276**, 14004–14013.
el-Deiry WS, Tokino T, Velculescu VE, Levy DB, Parsons R, Trent JM, Lin D, Mercer WE, Kinzler KW and Vogelstein B. (1993). *Cell*, **75**, 817–825.
Engelhardt OG, Ullrich E, Kochs G and Haller O. (2001). *Exp. Cell Res.*, **271**, 286–295.
Gostissa M, Hengstermann A, Fogal V, Sandy P, Schwarz SE, Scheffner M and Del Sal G. (1999). *EMBO J.*, **18**, 6462–6471.
Haluska Jr P, Saleem A, Rasheed Z, Ahmed F, Su EW, Liu LF and Rubin EH. (1999). *Nucleic Acids Res.*, **27**, 2538–2544.
Harper JW, Adami GR, Wei N, Keyomarsi K and Elledge SJ. (1993). *Cell*, **75**, 805–816.
Kahyo T, Nishida T and Yasuda H. (2001). *Mol. Cell*, **8**, 713–718.
Kingma PS and Osheroff N. (1998). *Biochim. Biophys. Acta*, **1400**, 223–232.
Klibanov SA, O'Hagan HM and Ljungman M. (2001). *J. Cell Sci.*, **114**, 1867–1873.
Ko LJ and Prives C. (1996). *Genes Dev.*, **10**, 1054–1072.
Lane DP. (1992). *Nature*, **358**, 15–16.
Lassus P, Ferlin M, Piette J and Hibner U. (1996). *EMBO J.*, **15**, 4566–4573.
Levine AJ. (1997). *Cell*, **88**, 323–331.
Mann KK and Miller Jr WH. (2004). *Cancer Cell*, **5**, 307–309.
Matthews JM and Sunde M. (2002). *IUBMB Life*, **54**, 351–355.
Miyashita T and Reed JC. (1995). *Cell*, **80**, 293–299.
Oyanagi H, Takenaka K, Ishikawa S, Kawano Y, Adachi Y, Ueda K, Wada H and Tanaka F. (2004). *Lung Cancer*, **46**, 21–28.
Rajendra R, Malegaonkar D, Pungaliya P, Marshall H, Rasheed Z, Brownell J, Liu LF, Lutzker S, Saleem A and Rubin EH. (2004). *J. Biol. Chem.*, **279**, 36440–36444.
Rasheed ZA, Saleem A, Ravee Y, Pandolfi PP and Rubin EH. (2002). *Exp. Cell Res.*, **277**, 152–160.
Rodriguez MS, Desterro JM, Lain S, Midgley CA, Lane DP and Hay RT. (1999). *EMBO J.*, **18**, 6455–6461.
Saleem A, Dutta J, Malegaonkar D, Rasheed F, Rasheed Z, Rajendra R, Marshall H, Luo M, Li H and Rubin EH. (2004). *Oncogene*, **23**, 5293–5300.
Schlehofer JR. (1994). *Mutat. Res.*, **305**, 303–313.
Secombe J and Parkhurst SM. (2004). *J. Biol. Chem.*, **279**, 17126–17133.
Sionov RV and Haupt Y. (1999). *Oncogene*, **18**, 6145–6157.
Vogelstein B, Lane D and Levine AJ. (2000). *Nature*, **408**, 307–310.
Vojtek AB, Hollenberg SM and Cooper JA. (1993). *Cell*, **74**, 205–214.
Watanabe K, Ozaki T, Nakagawa T, Miyazaki K, Takahashi M, Hosoda M, Hayashi S, Todo S and Nakagawara A. (2002). *J. Biol. Chem.*, **277**, 15113–15123.
Weger S, Hammer E and Engstler M. (2003). *Exp. Cell Res.*, **290**, 13–27.
Weger S, Hammer E and Heilbronn R. (2002). *J. Gen. Virol.*, **83**, 511–516.
Yamaki M, Isono K, Takada Y, Abe K, Akasaka T, Tanzawa H and Koseki H. (2002). *Gene*, **288**, 103–110.
Zhou R, Wen H and Ao SZ. (1999). *Gene*, **235**, 93–101.

Available online at www.sciencedirect.com
SCIENCE DIRECT®
Cancer Letters 228 (2005) 29–35
CANCER Letters
www.elsevier.com/locate/canlet

Mini-review

Functional implication of p73 protein stability in neuronal cell survival and death

Toshinori Ozaki[a], Mitsuchika Hosoda[a,b], Kou Miyazaki[a], Syunji Hayashi[a,b], Ken-ichi Watanabe[a,b], Takahito Nakagawa[a,b], Akira Nakagawara[a,*]

[a]*Division of Biochemistry, Chiba Cancer Center Research Institute, 666-2 Nitona, Chuoh-ku, Chiba 260-8717, Japan*
[b]*Department of General Surgery, Hokkaido University School of Medicine, Sapporo 060-8638, Japan*

Received 26 November 2004; accepted 2 December 2004

Abstract

p73, a newly identified member of *p53* family, locates at human chromosome 1p36.2-3, a region which is frequently deleted in a wide variety of human tumors including neuroblastoma. p73 is induced to be accumulated in response to a subset of DNA damaging agents such as cisplatin, and thereby promoting G1/S cell cycle arrest and/or apoptosis. Since the expression levels of p73 are kept extremely low under normal conditions, stabilization of p73 is critical for its effects on cell growth inhibition and apoptosis. Indeed, p73 is induced at protein level in SH-SY5Y neuroblastoma cells exposed to cisplatin. Several lines of evidence indicate that stress-induced post-translational modifications of p73 such as phosphorylation and acetylation lead to a marked extension of its half-life. p73 stability is regulated at least in part by proteasome-dependent degradation pathway, however, MDM2 which mediates ubiquitination and subsequent degradation of p53 by the 26S proteasome, does not promote the proteolytic degradation of p73, implying that the protein stability of p73 is regulated through a pathway distinct from that of p53. Although little is known about the regulation of p73 turnover, we are now beginning to understand the regulatory mechanisms by which p73 is induced to be stabilized in response to apoptotic stimuli, and exerts its pro-apoptotic activity. In this review, we discuss about the cellular proteins implicated in the stability control of p73.

Keywords: E3 ubiquitin ligase; MDM2; Neuroblastoma; p53; p73; p63; Proteasome; Ubiquitination; UFD2a

1. Introduction

p73 belongs to the tumor suppressor p53 family including p53, p73 and p63 [1,2]. As expected from their structural similarity, particularly in the central sequence-specific DNA-binding domain (over 60% amino acid sequence identity), p73 displays several p53-like properties. Analogous to p53, p73 can transactivate a large number of p53-responsive genes such as $p21^{WAF1}$ and *Bax*, and thereby inducing G1/S cell cycle arrest and/or apoptosis in a variety of cancerous cells [3]. *p73* gene has been mapped to human chromosome 1p36.2-3, a region which is frequently lost in neuroblastoma and other types of

* Corresponding author. Tel.: +81 43 264 5431; fax: +81 43 265 4459.
E-mail address: akiranak@chiba-cc.jp (A. Nakagawara).

0304-3835/$ - see front matter © 2005 Elsevier Ireland Ltd. All rights reserved.
doi:10.1016/j.canlet.2004.12.050

tumors [1]. In a sharp contrast to p53, however, p73 is rarely mutated in human tumors including neuroblastoma despite an extensive search [4], and the loss of p73 does not predispose mice to cancer [5], suggesting that p73 does not function as a classic Knudson-type tumor suppressor. Recently, it has been demonstrated that the p53-dependent apoptosis requires the indirect contribution of at least one of the other p53 family members, p73 or p63 [6], whereas p73 is sufficient to induce apoptosis in the absence of p53 [7,8]. Thus, it is likely that p73 cooperates with p53 to induce apoptosis and/or exerts its pro-apoptotic activity in a p53-independent manner. These findings have emphasized the functional importance of p73 in the regulation of apoptotic response, and attracted considerable attention. In particular, p73 is regarded as an important cell fate determinant of neuroblastoma in response to apoptotic stimuli, because wild-type p53 lacks its intact function due to its abnormal cytoplasmic localization in neuroblastoma [9].

Unlike p53, p73 is expressed as multiple variants with varying COOH-terminal extensions (TA isoforms) and lacking NH_2-terminal transactivation domain (ΔN isoforms), arising from alternative splicing and promoter usage, respectively (Fig. 1) [3]. Among them, ΔNp73 has an oncogenic potential [10], and exhibits a dominant-negative behavior toward TAp73 as well as p53 [5,11]. Consistent with this notion, the expression levels of ΔNp73 are closely associated with poor prognosis in human tumors including neuroblastoma [12,13]. Intriguingly, we and others found that p73 directly transactivates the expression of ΔNp73, suggesting that there exists a negative feedback regulation of p73 by ΔNp73 to modulate cell survival and death [14,15].

Steady-state expression levels of endogenous p73 are maintained at extremely low level under normal conditions, keeping this dangerous protein in an inactive state. In response to a subset of genotoxic stresses including oncotoxic drug cisplatin and ionizing radiation, however, p73 is induced to be accumulated at protein level, and the stabilization of p73 results in either G1/S cell cycle arrest or commitment to death through apoptosis [16]. Thus, stabilization of p73 is directly linked with its function. Several pieces of evidence suggest that the protein stability of p73 is regulated through a pathway distinct from that of p53 [8,17]. Although p73 protein stability is regulated at least in part by proteasomal degradation [17,18], it remains still unknown whether the proteasome-mediated degradation system is the main degradation route of p73. In this review, we will discuss about the cellular proteins regulating the p73 stability and how they affect its stability and activity.

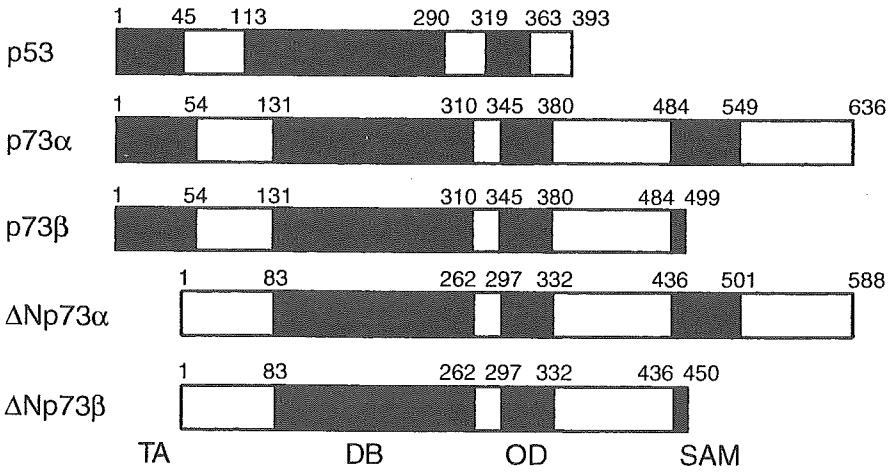

Fig. 1. Structural comparison between p53 and p73. p73α and p73β are generated by alternative splicing. Alternative promoter usage gives rise to ΔNp73α and ΔNp73β. The domains indicated are: a transactivation domain (TA), a DNA-binding domain (DB), an oligomerization domain (OD) and a sterile alpha motif domain (SAM).

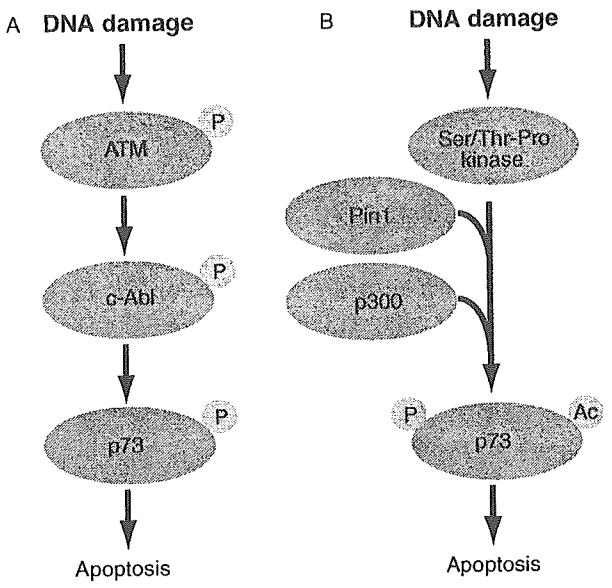

Fig. 2. Chemical modification enhances the stability as well as pro-apoptotic activity of p73 in response to DNA damage. (A) In response to DNA damage, nuclear nonreceptor tyrosine kinase c-Abl is activated by ATM, and thereby phosphorylating p73 at Tyr-99. (B) Pin1 recognizes phosphorylated serine or threonine residues of p73 which can be catalyzed by as yet unidentified Ser/Thr-Pro-directed kinase(s), and enhances its acetylation by p300.

2. Chemical modifications which make p73 stable

Genotoxic stresses including cisplatin treatment and ionizing radiation prolong the half-life of p73 and enhance its pro-apoptotic activity in a pathway dependent on nuclear nonreceptor tyrosine kinase c-Abl [19–21]. According to those results, c-Abl interacts with p73 through the SH3 domain of c-Abl and the p73 PXXP motif, and directly phosphorylates p73 at Tyr-99. Consistent with this notion, p73 is not induced to be accumulated in c-Abl-deficient cells in response to cisplatin (Fig. 2A) [19]. Intriguingly, Ben-Yehoyada et al. found that ionizing radiation induces the tyrosine phosphorylation as well as stabilization of p73 in a c-Abl-dependent manner, and the phosphorylated forms of p73 become associated with the nuclear matrix, suggesting that c-Abl-mediated nuclear redistribution of p73 might play a critical role in the regulation of p73 function [22]. They also described that the amounts of p73 associated with nuclear matrix are increased in the presence of proteasome inhibitor such as MG-132. Alternatively, cisplatin treatment promotes the interaction between p73 and protein kinase Cδ catalytic fragment (PKCδCF) [23]. PKCδCF phosphorylates p73 at Ser-289, and increases its stability. Since PKCδCF enhances the catalytic activity of c-Abl, it is likely that c-Abl could act as a second signal in the functional interaction with p73. Recently, Gonzalez et al. reported that cisplatin-induced apoptosis is associated with the phosphorylation of p73 at Ser-47 catalyzed by Chk1 [24]. Chk1-mediated phosphorylation might convert a latent form of p73 to an active one. Additionally, p73 is phosphorylated at Thr-86 by CDK complexes in a cell cycle-dependent manner [25]. In a sharp contrast to Chk1, the CDK-mediated phosphorylation causes a significant inhibition of the transcriptional activity of p73. Under their experimental conditions, CDK complexes have negligible effect on the amounts of p73.

In addition to the DNA-damage-induced phosphorylation of p73, p73 is regulated by acetylation. Previously, it has been demonstrated that p300 interacts with the NH_2-terminal region of p73, and enhances its pro-apoptotic activity [26]. It is worth noting that doxorubicin treatment induces the acetylation of p73 at Lys-321, Lys-327 and Lys-331 and this acetylation is mediated by p300 in a c-Abl-dependent manner [27]. Based on these results, acetylated form of p73 has a pro-apoptotic activity, whereas nonacetylatable p73 fails to promote apoptosis. Moreover, Mantovani et al. found that p300-mediated acetylation of p73 is enhanced by prolyl isomerase Pin1, and promotes the stabilization of p73 [28]. Pin1 binds to the phosphorylated serine or threonine residue followed by proline of p73, and induces its conformational shift to stimulate the interaction between p73 and p300 (Fig. 2B). Thus, the identification of Ser/Thr kinase(s) required for the phosphorylation of Pin1-binding site on p73 is important to clarify a molecular mechanism underlying the DNA damage-induced stabilization of p73.

3. Ubiquitin-mediated proteolysis of p73

p73 level is dependent on a balance between protein synthesis and degradation. As described by Lee and La Thangue [18], the steady-state expression levels of p73 are significantly increased in the presence of proteasome inhibitor such as LLnL,

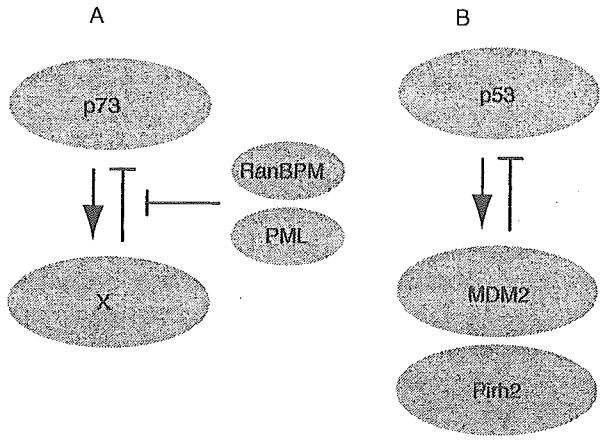

Fig. 3. Ubiquitination-dependent degradation pathway of p73 is distinct from that used for p53. (A) Ubiquitination of p73 could be mediated by p73-induced gene product(s), and significantly inhibited by RanBPM and/or PML. (B) p53-induced E3 ubiquitin ligases MDM2 and Pirh2 promote the ubiquitination and subsequent degradation of p53 by 26S proteasome, however, they have negligible effect on the ubiquitination level of p73.

suggesting that p73 turnover is regulated at least in part by a ubiquitin-dependent proteasome pathway. They also showed that the COOH-terminal extension of p73α is involved in the regulation of protein stability through a pathway that is sensitive to proteasome inhibitor. Recently, we found that RanBPM binds to the extreme COOH-terminal region of p73α, and inhibits its ubiquitination [29]. Of note, Bernassola et al. reported that PML promotes the p300-mediated acetylation of p73, and reduces its ubiquitination levels by competition between acetylation and ubiquitination [30]. In addition, Wu et al. described that the transcriptional activity of p73 is required for its rapid degradation, indicating that the direct transcriptional target(s) of p73 could have an ability to induce its proteolytic degradation (Fig. 3A) [31]. In accordance with this notion, ΔNp73 which lacks the NH_2-terminal transactivation domain, is much more stable than wild-type p73. MDM2 which acts as an E3 ubiquitin ligase for p53, promotes the ubiquitination and subsequent degradation of p53 [32–34]. MDM2 is transcriptionally activated by p53, forming an autoregulatory feedback loop with p53 to tightly regulate its expression levels (Fig. 3B). Similar to p53, p73 stimulates the transcription of MDM2. MDM2 interacts with the NH_2-terminal transactivation domain of p73 and abrogates its transcriptional activity as well as pro-apoptotic function, whereas it fails to mediate the proteolytic degradation of p73 [35,36]. Like p73, p63 is degraded by a proteasome-dependent pathway, however, MDM2 increases the steady-state level of intracellular p63 [37]. Another p53-induced E3 ubiquitin ligase Pirh2 which promotes p53 degradation (Fig. 3B), has no detectable effect on p73 stability [31,38], suggesting that p73 degradation might be mediated by an as yet unidentified E3 ubiquitin ligase(s) distinct from that used for p53 degradation. Intriguingly, Toh et al. described that c-Jun fails to interact with p73 but prolongs the half-life of p73 by preventing its proteasome-dependent degradation [39]. According to those results, the transactivation function of c-Jun is required for the c-Jun-mediated stabilization of p73. Thus, it is likely that c-Jun activates its transcriptional target(s) implicated in the regulation of p73 stability.

4. Ubiquitination-independent degradation of p73

In addition to the ubiquitin-mediated proteasome pathway, p73 degradation is regulated in a ubiquitination-independent manner. Cyclin G which belongs to the cyclin family, has been shown to be one of the transcriptional target genes of p53 [40]. Recently, Ohtsuka et al. demonstrated that cyclin G interacts with p73 and promotes its down-regulation at protein level [41]. siRNA-mediated knock-down of the endogenous cyclin G results in a significant accumulation of p73 in response to DNA damage. Unexpectedly, cyclin G does not increase the amounts of the ubiquitinated forms of p73, suggesting that cyclin G-mediated destabilization of p73 might be regulated through a pathway distinct from the ubiquitination-dependent degradation system. However, the precise regulatory mechanism of p73 stability by cyclin G remains to be elusive.

5. Viral oncoproteins

As described by Marin et al. [42], HEK293 human embryonic kidney and COS monkey kidney cells express the higher levels of p73 as compared with the other cell lines. HEK293 and COS cells are transformed with viral oncoproteins such as adenovirus E1B and

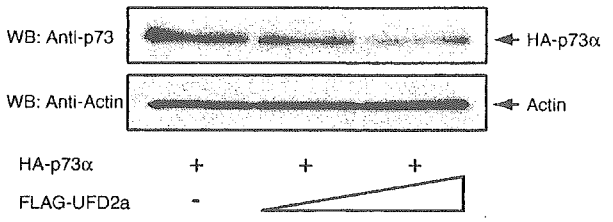

Fig. 4. Down-regulation of p73 by UFD2a. U2OS cells were transiently co-transfected with the indicated combinations of the expression plasmids. Forty-eight hours after transfection, whole cell lysates were prepared and subjected to Western blot analysis (WB) with the indicated antibodies.

simian virus 40 (SV40) T antigen, respectively. In addition, Lemasson and Nyborg reported that HTLV-1-transformed cells express a high level of p73, whereas p73 is undetectable in uninfected T-cell lines [43]. Viral oncoprotein Tax which is encoded by HTLV-I, has an ability to enhance the stability of p73. Since these viral oncoproteins do not interact directly with p73, as yet unidentified indirect mechanism(s) appears to contribute to maintain the higher levels of p73 in those transformed cells. Considering that adenovirus E1A binds to p300 and inhibits its E3/E4 ubiquitin ligase activity to stabilize p53 [44], it is plausible that viral oncoproteins such as E1B, T antigen and Tax could inhibit the enzymatic activity of unidentified E3/E4 ubiquitin ligase for p73 through the physical interaction, and thereby protecting p73 from ubiquitination-mediated proteolytic degradation.

6. Interaction between p73 and UFD2a in human neuroblastoma cell lines

We have previously identified a homozygously deleted region at 1p36.2-p36.3 in neuroblastoma cell line NB-C201 [45]. Within this region, there exist six genes including *DFF45*, *PGD*, *CORT*, *UFD2a*, *KIF1B*-β and *PEX14*. Among them, UFD2a which belongs to the U-box-type ubiquitin ligase family, has an E3 as well as E4 ubiquitin ligase activity [46,47]. It has been shown that UFD2a is implicated in cell survival under a certain stress condition [46]. In response to apoptotic stimuli, UFD2a is cleaved by caspase 6 or granzyme B, and its enzymatic activity is markedly impaired [48]. It is, thus, tempting to speculate that UFD2a might participate in the regulation of cell survival and death.

Recently, we have found that, during the cisplatin-mediated apoptosis in SH-SY5Y neuroblastoma cells, UFD2a is down-regulated at protein level in association with a significant accumulation of p73. Ectopic expression of UFD2a results in a reduction of p73 (Fig. 4), and this observation is supported by a decrease in a half-life of p73 in UFD2a-expressing cells. This is consistent with our additional findings showing that UFD2a inhibits the p73-mediated transcriptional activation and apoptosis [Hosoda et al., manuscript in preparation]. Although it is not known whether UFD2a-mediated degradation of p73 could be regulated in a ubiquitination-dependent manner, it is conceivable that down-regulation of UFD2a in response to cisplatin might augment the p73-dependent apoptosis, and thereby providing a novel strategy for anticancer treatment.

7. Conclusion

In contrast to other types of human tumors, *p53* is rarely mutated in neuroblastoma, however, the aberrant cytoplasmic retention of wild-type p53 renders it nonfunctional. Since p73 has an ability to induce tumor cell apoptosis irrespective of *p53* status, it is likely that p73 is a pivotal player in apoptotic response, particularly in tumors such as neuroblastoma lacking functional p53. Accumulating evidence strongly suggests that p73 is regulated through a pathway distinct from that of p53. In this respect, it is necessary to clarify signaling pathways which specifically regulate the activity as well as stability of p73 in response to apoptotic stimuli.

References

[1] M. Kaghad, H. Bonnet, A. Yang, L. Creancier, J.C. Biscan, A. Valent, et al., Monoallelically expressed gene related to p53 at 1p36, a region frequently deleted in neuroblastoma and other human cancers, Cell 90 (1997) 809–819.
[2] A. Yang, M. Kaghad, Y. Wang, E. Gillett, M.D. Fleming, V. Dotsch, et al., p63, a p53 homolog at 3q27-29, encodes multiple products with transactivating, death-inducing, and dominant-negative activities, Mol. Cell 2 (1998) 305–316.
[3] G. Melino, V. De Laurenzi, K.H. Vousden, p73: friend or foe in tumorigenesis, Nat. Rev. Cancer 2 (2002) 605–615.

[4] S. Ikawa, A. Nakagawara, Y. Ikawa, p53 family genes: structural comparison, expression and mutation, Cell Death Differ. 6 (1999) 1154–1161.
[5] A. Yang, N. Walker, R. Bronson, M. Kaghad, M. Oosterwegel, J. Bonnin, et al., Caput, p73-deficient mice have neurological, pheromonal and inflammatory defects but lack spontaneous tumours, Nature 404 (2000) 99–103.
[6] E.R. Flores, K.Y. Tsai, D. Crowley, S. Sengupta, A. Yang, F. McKeon, T. Jacks, p63 and p73 are required for p53-dependent apoptosis in response to DNA damage, Nature 416 (2002) 560–564.
[7] C.A. Jost, M.C. Marin, W.G. Kaelin Jr., p73 is a simian p53-related protein that can induce apoptosis, Nature 389 (1997) 191–194.
[8] X. Zeng, L. Chen, C.A. Jost, R. Maya, D. Keller, X. Wang, et al., MDM2 suppresses p73 function without promoting p73 degradation, Mol. Cell Biol. 19 (1999) 3257–3266.
[9] U.M. Moll, M. LaQuaglia, J. Benard, G. Riou, Wild type p53 protein undergoes cytoplasmic sequestration in undifferentiated neuroblastomas but not in differentiated tumors, Proc. Natl Acad. Sci. USA 92 (1995) 4407–4411.
[10] T. Stiewe, S. Zimmermann, A. Frilling, H. Esche, B.M. Putzer, Transactivation-deficient ΔTA-p73 acts as an oncogene, Cancer Res. 62 (2002) 3598–3602.
[11] C.D. Pozniak, S. Radinovic, A. Yang, F. McKeon, D.R. Kaplan, F.D. Miller, An anti-apoptotic role for the p53 family member, p73, during developmental neuron death, Science 289 (2000) 304–306.
[12] I. Casciano, K. Mazzocco, L. Boni, G. Pagnan, B. Banelli, G. Allemanni, et al., Expression of ΔNp73 is a molecular marker for adverse outcome in neuroblastoma patients, Cell Death Differ. 9 (2002) 246–251.
[13] A.I. Zaika, N. Slade, S.H. Erster, C. Sansome, T.W. Joseph, M. Pearl, U.M. Moll, ΔNp73 a dominant-negative inhibitor of wild-type p53 and TAp73, is up-regulated in human tumors, J. Exp. Med. 196 (2002) 765–780.
[14] T.J. Grob, U. Novak, C. Maisse, D. Barcaroli, A.U. Luthi, F. Pimia, A. Tobler, Human ΔNp73 regulates a dominant negative feedback loop for TAp73 and p53, Cell Death Differ. 8 (2001) 1213–1223.
[15] T. Nakagawa, M. Takahashi, T. Ozaki, K. Watanabe, S. Todo, H. Mizuguchi, et al., Autoinhibitory regulation of p73 by ΔNp73 to modulate cell survival and death through a p73-specific target element within the ΔNp73 promoter, Mol. Cell Biol. 22 (2002) 2575–2585.
[16] M.S. Irwin, K. Kondo, M.C. Marin, L.S. Cheng, W.C. Hahn, W.G. Kaelin Jr., Chemosensitivity linked to p73 function, Cancer Cell 3 (2003) 403–410.
[17] E. Balint, S. Bates, K.H. Vousden, Mdm2 binds p73α without targeting degradation, Oncogene 18 (1999) 3923–3929.
[18] C.W. Lee, N.B. La Thangue, Promoter specificity and stability control of the p53-related protein p73, Oncogene 18 (1999) 4171–4181.
[19] J. Gong, A. Costanzo, H.G. Yang, G. Melino, W.G. Kaelin Jr., M. Levrero, J.Y.J. Wang, The tyrosine kinase c-Abl regulates p73 in apoptotic response to cisplatin-induced DNA damage, Nature 399 (1999) 806–809.
[20] R. Agami, G. Blandino, M. Oren, Y. Shaul, Interaction of c-Abl and p73α and their collaboration to induce apoptosis, Nature 399 (1999) 809–813.
[21] Z.M. Yuan, H. Shioya, T. Ishiko, X. Sun, J. Gu, Y.Y. Huang, et al., p73 is regulated by tyrosine kinase c-Abl in the apoptotic response to DNA damage, Nature 399 (1999) 814–817.
[22] M. Ben-Yehoyada, I. Ben-Dor, Y. Shaul, c-Abl tyrosine kinase selectively regulates p73 nuclear matrix association, J. Biol. Chem. 278 (2003) 34475–34482.
[23] J. Ren, R. Datta, H. Shioya, Y. Li, E. Oki, V. Biedermann, et al., p73β is regulated by protein kinase Cδ catalytic fragment generated in the apoptotic response to DNA damage, J. Biol. Chem. 277 (2002) 33758–33765.
[24] S. Gonzalez, C. Prives, C. Cordon-Cardo, p73α regulation by Chk1 in response to DNA damage, Mol. Cell. Biol. 23 (2003) 8161–8171.
[25] C. Gaiddon, M. Lokshin, I. Gross, D. Levasseur, Y. Taya, J.P. Loeffler, C. Prives, Cyclin-dependent kinases phosphorylate p73 at threonine 86 in a cell cycle-dependent manner and negatively regulate p73, J. Biol. Chem. 278 (2003) 27421–27431.
[26] X. Zeng, X. Li, A. Miller, Z. Yuan, W. Yuan, R.P. Kwok, et al., The N-terminal domain of p73 interacts with the CH1 domain of p300/CBP binding protein and mediates transcriptional and apoptosis, Mol. Cell. Biol. 20 (2001) 1299–1310.
[27] A. Costanzo, P. Merlo, N. Pediconi, M. Fulco, V. Sartorelli, P.A. Cole, et al., DNA damage-dependent acetylation of p73 dictates the selective activation of apoptotic target genes, Mol. Cell 9 (2002) 175–186.
[28] F. Mantovani, S. Piazza, M. Gostissa, S. Strano, P. Zacchi, R. Mantovani, et al., Pin1 links the activities of c-Abl and p300 in regulating p73 function, Mol. Cell 14 (2004) 625–636.
[29] S. Kramer, T. Ozaki, K. Miyazaki, C. Kato, T. Hanamoto, A. Nakagawara, Protein stability and function of p73 are modulated by a physical interaction with RanBPM in mammalian cultured cells, Oncogene 27 (2005) 938–944.
[30] F. Bernassola, P. Salomoni, A. Oberst, C.J. Di Como, M. Pagano, G. Melino, P. Paolo Pandolfi, Ubiquitin-dependent degradation of p73 is inhibited by PML, J. Exp. Med. 199 (2004) 1545–1557.
[31] L. Wu, H. Zhu, L. Nie, C.G. Maki, A link between p73 transcriptional activity and p73 degradation, Oncogene 23 (2004) 4032–4036.
[32] Y. Haupt, R. Maya, A. Kazaz, M. Oren, Mdm2 promotes the rapid degradation of p53, Nature 387 (1997) 296–299.
[33] M.H.G. Kubbutat, S.N. Jones, K.H. Vousden, Regulation of p53 stability by mdm2, Nature 387 (1997) 299–303.
[34] R. Honda, H. Tanaka, H. Yasuda, Oncoprotein MDM2 is a ubiquitin ligase E3 for tumor suppressor p53, Fed. Eur. Biochem. Soc. Lett. 420 (1997) 25–27.
[35] X. Zeng, L. Chen, C.A. Jost, R. Maya, D. Keller, X. Wang, et al., MDM2 suppresses p73 function without promoting p73 degradation, Mol. Cell. Biol. 19 (1999) 3257–3266.

[36] E. Balint, S. Bates, K.H. Vousden, Mdm2 binds p73α without targeting degradation, Oncogene 18 (1999) 3923–3929.
[37] V. Calabro, G. Mansueto, T. Parisi, M. Vivo, R.A. Calogero, G. La Mantia, The human MDM2 oncoprotein increases the transcriptional activity and the protein level of the p53 homolog p63, J. Biol. Chem. 277 (2002) 2674–2681.
[38] R.P. Leng, Y. Lin, W. Ma, H. Wu, B. Lemmers, S. Chung, et al., Pirh2, a p53-induced ubiquitin-protein ligase, promotes p53 degradation, Cell 112 (2003) 779–791.
[39] W.H. Toh, M.M. Siddique, L. Boominathan, K.W. Lin, K. Sabapathy, c-Jun regulates the stability and activity of the p53 homologue, p73, J. Biol. Chem. 22 (2004) 44713–44722.
[40] K. Okamoto, D. Beach, Cyclin G is a transcriptional target of the p53 tumor suppressor protein, Eur. Mol. Biol. Org. J. 13 (1994) 4816–4822.
[41] T. Ohtsuka, H. Ryu, Y.A. Minamishima, A. Ryo, S.W. Lee, Modulation of p53 and p73 levels by cyclin G: implication of a negative feedback regulation, Oncogene 22 (2003) 1678–1687.
[42] M.C. Marin, C.A. Jost, M. Irwin, J.A. Decaprio, D. Caput, W.G. Kaelin Jr., Viral oncoproteins discriminate between p53 and the p53 homolog p73, Mol. Cell. Biol. 18 (1998) 6316–6324.
[43] I. Lemasson, J.K. Nyborg, Human T-cell leukemia virus type I Tax repression of p73β is mediated through competition for the C/H1 domain of CBP, J. Biol. Chem. 276 (2001) 15720–15727.
[44] S.R. Grossman, M.E. Deato, C. Brignone, H.M. Chan, A.L. Kung, H. Tagami, et al., Polyubiquitination of p53 by a ubiquitin ligase activity of p300, Science 300 (2003) 342–344.
[45] M. Ohira, H. Kageyama, M. Mihara, S. Furuta, T. Machida, T. Shishikura, et al., Identification and characterization of a 500-kb homozygously deleted region at 1p36.2-p36.3 in a neuroblastoma cell line, Oncogene 19 (2000) 4302–4307.
[46] M. Koegl, T. Hoppe, S. Schlenker, H.D. Ulrich, T.U. Mayer, S. Jentsch, A novel ubiquitination factor, E4, is involved in multiubiquitin chain assembly, Cell 96 (1999) 635–644.
[47] S. Hatakeyama, M. Yada, M. Matsumoto, N. Ishida, K.I. Nakayama, U box proteins as a new family of ubiquitin-protein ligases, J. Biol. Chem. 276 (2001) 33111–33120.
[48] J.A. Mahoney, J.A. Odin, S.M. White, D. Shaffer, A. Koff, L. Casciola-Rosen, The human homologue of the yeast polyubiquitination factor Ufd2p is cleaved by caspase 6 and granzyme B during apoptosis, Biochem. J. 361 (2002) 587–595.